ELSEVIER

Journal of Biomechanics 33 (2000) 487–491

JOURNAL OF BIOMECHANICS

www.elsevier.com/locate/jbiomech

Technical note

A new kinematic model of pro- and supination of the human forearm☆

A.M. Weinberg[a], I.T. Pietsch[b,*], M.B. Helm[b], J. Hesselbach[b], H. Tscherne[a]

[a]*Trauma Department of the Medical University of Hanover (MHH), Germany*

[b]*Institute of Machine Tools and Production Engineering, Technical University of Braunschweig, D-38106 Braunschweig, Germany*

Accepted 12 October 1999

Abstract

We introduce a new kinematic model describing the motion of the human forearm bones, ulna and radius, during forearm rotation. During this motion between the two forearm extrem-positions, referred to as supination (palm up) and pronation (palm down), effects occur, that cannot be explained by the the established kinematic model of R. Fick from 1904. Especially, the motion of the ulna is not properly reproduced by Fick's model. During forearm rotation an evasive motion of the ulna is observed by various authors, using magnetic resonance imaging (MRI) technology. Our new kinematic model also simulates this evasive motion. Furthermore, the model is enlarged to include angulations of the forearm bones. Using these results the influence of forearm fractures on the range of forearm motion can be predicted. This knowledge can be used by surgeons to choose the optimal therapy in re-establishing free forearm mobility.

1. Introduction

Performance of the pro- and supination motion is important to the human capability of acting in a fine-motorial way, which is necessary in an increasing number of technical jobs and everyday life.

Forearm fractures sometimes result in broken bones healing in angulated positions (Nilsson and Obrant, 1977; Kuderna, 1980). Today, a physicians evaluation of the neccesity to operate is based on a small amount of available information and clinical studies. As a result of this lack of knowledge many patients with fresh fractures are operated on, to force the broken bone in a certain position whereas the physician is not sure about the effect of the current bone-position (Weiner, 1981).

This situation motivated our research with the goal of presenting a kinematic model, which predicts the limitation of motion caused by a known angulation. With this knowledge unnecessary operations can be prevented and the results of the necessary ones can be improved.

Forearm motion research began in the early 20th century. Fick (1904) presented the first kinematic model describing forearm motion, which is still used in many publications (e.g. Kuderna, 1980; Green and Swiontkowski, 1998). The model basis requires the ulna to remain fixed during the whole rotation, as shown in the left drawing of Fig. 1. According to Fick, the hand should not stay parallel during rotation, which is easily refuted by personal experience. The right drawing in Fig. 1 depicts the evasive motion of ulna and radius, which ensures the parallelism of the hand to the elbow.

2. Methods

The new kinematic model uses a database of MRI-scans of the pro- and supination that were evaluated in 30 healthy forearms for kinematic behavior (Weinberg et al., 1997). The scans were taken at different sections of the forearm for several pro- and supination-angles. Spatial motion of the bones involved in pro- and supination require a spatial mechanism.

2.1. Kinematic model for healthy forearm bones

The degree of freedom F (d.o.f.) for a general spatial mechanism is given by

$$F = 6(n - g - 1) + \sum_{i=1}^{n} f_i, \tag{1}$$

☆The research program is supported by the German Research Foundation (DFG).

* Corresponding author.

E-mail address: i.pietsch@tu-bs.de (I.T. Pietsch)

0021-9290/00/$ - see front matter
PII: S0021-9290(99)00195-5

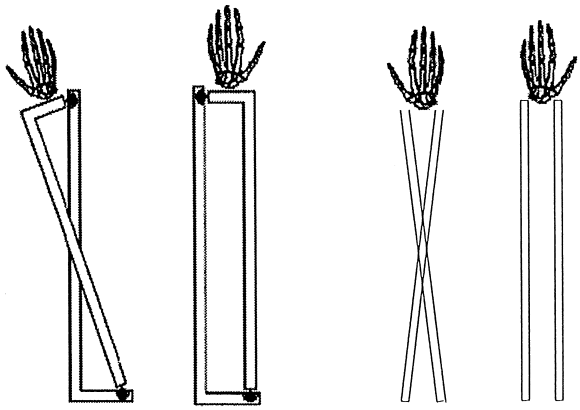

Fig. 1. Fick's model from 1904 (left) does not allow the hand to stay parallel to the elbow during forearm rotation. Evasive movement of ulna and radius to ensure parallelism of hand and elbow as performed in reality (right).

where n is the number of elements, g the number of joints and f_i the d.o.f. of each joint.

We chose a closed kinematic chain with four joints as our model. With $n = g = 4$ and the positive gear constraint of $F = 1$, we find using (1) that,

$$\sum_{i=1}^{n} f_i = 1 - 6(4 - 4 - 1) = 7 \tag{2}$$

which means distribution of seven d.o.f. among the four joints. Fig. 2 depicts our mechanism. It has one spherical joint (d.o.f. = 3) on the proximal end of the ulna (1) and one rotational joint (d.o.f. = 1) on the ulna's distal end (2). The radius has one cardanic joint (d.o.f. = 2) on the distal end (3) and a prismatic joint (d.o.f. = 1) on the proximal end (4) (Kerle and Frindt, 1997).

For the mathematical formulation of this system, a closed vector-chain is introduced in Fig. 2. The angle α indicates the actual position of pro- or supination. Therefore, the total d.o.f. of the system is one, it is now possible to find exactly one clear position of the mechanism for every angle α. The length of the bones (the length of the vectors $\mathbf{r}_1$ and $\mathbf{r}_3$) is called l_1 and the distance between their centers at their ends (the length of the vectors $\mathbf{r}_2$ and $\mathbf{r}_4$) is called l_2.

$$|\mathbf{r}_1| = |\mathbf{r}_3| = l_1,$$

$$|\mathbf{r}_2| = |\mathbf{r}_4| = l_2,$$

$$|\mathbf{r}_5| = f(\alpha). \tag{3}$$

The whole set of vectors r_i describes a closed kinematic chain. From this condition arises the equation

$$\sum_{i=1}^{5} \mathbf{r}_i = \sum_{i=1}^{5} \begin{pmatrix} r_{x_i} \\ r_{y_i} \\ r_{z_i} \end{pmatrix} = \mathbf{0}. \tag{4}$$

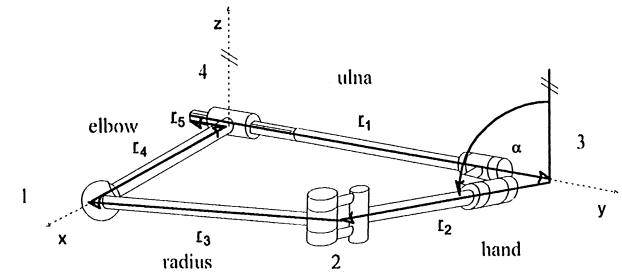

Fig. 2. Kinematic model of the forearm consisting of four elements, depicted as a vector chain.

The initial conditions in supination position ($\alpha = 90^\circ := \alpha_s$) are:

$$\mathbf{r}_1(\alpha_s) = \mathbf{r}_1(\alpha) = l_1 \begin{pmatrix} 0 \\ 1 \\ 0 \end{pmatrix}, \tag{5}$$

$$\mathbf{r}_2(\alpha_s) = l_2 \begin{pmatrix} 1 \\ 0 \\ 0 \end{pmatrix}, \tag{6}$$

$$\mathbf{r}_3(\alpha_s) = l_1 \begin{pmatrix} 0 \\ -1 \\ 0 \end{pmatrix}, \tag{7}$$

$$\mathbf{r}_4(\alpha_s) = \mathbf{r}_4(\alpha) = l_2 \begin{pmatrix} -1 \\ 0 \\ 0 \end{pmatrix}, \tag{8}$$

$$\mathbf{r}_5(\alpha_s) = \mathbf{0}. \tag{9}$$

The condition

$$(\mathbf{r}_2(\alpha) \,||\, \mathbf{r}_4(\alpha)) \wedge (\mathbf{r}_2(\alpha) \perp \mathbf{r}_1(\alpha)) \tag{10}$$

yields

$$\mathbf{r}_2(\alpha) = l_2 \begin{pmatrix} \sin(\alpha) \\ 0 \\ \cos(\alpha) \end{pmatrix}. \tag{11}$$

$\mathbf{r}_3$ can be determined by making use of

$$r_{x_2}(\alpha) + r_{x_3}(\alpha) = l_2 \tag{12}$$

and

$$r_{z_2}(\alpha) + r_{z_3}(\alpha) = 0. \tag{13}$$

With (12) and (11), respectively, (13) and (11) we obtain

$$r_{x_3}(\alpha) = l_2(1 - \sin(\alpha)) \tag{14}$$

and

$$r_{z_3}(\alpha) = -l_2 \cos(\alpha). \tag{15}$$

Eqs. (14) and (15), the magnitude of $\mathbf{r}_3(\alpha)$

$$|\mathbf{r}_3(\alpha)| = \sqrt{r_{x_3}^2 + r_{y_3}^2 + r_{z_3}^2}, \tag{16}$$

together with (7) results in

$$\mathbf{r}_3(\alpha) = l_2 \begin{pmatrix} 1 - \sin(\alpha) \\ -\sqrt{\dfrac{l_1^2}{l_2^2} - 2(1 - \sin(\alpha))} \\ -\cos(\alpha) \end{pmatrix}. \tag{17}$$

Fig. 2 sets forth that $r_{x_5}(\alpha) = r_{z_5}(\alpha) = 0$, because of the prismatic joint that allows only motions in the direction of the y-axis. In order to meet

$$\mathbf{r}_2(\alpha) \,||\, \mathbf{r}_4(\alpha), \tag{18}$$

r_{y_5} complies with

$$r_{y_5}(\alpha) = r_{y_1}(\alpha) + r_{y3}(\alpha). \tag{19}$$

Hence,

$$r_5(\alpha) = l_2 \begin{pmatrix} 0 \\ \dfrac{l_1}{l_2} - \sqrt{\dfrac{l_1^2}{l_2^2} - 2(1 - \sin(\alpha))} \\ 0 \end{pmatrix}. \tag{20}$$

2.2. Angulated bones

The basic idea of predicting the influence of angulations on the range of forearm motion is the calculation of the minimal distance between the two bones of the healthy forearm and setting that equal to the minimum allowable distance of the angulated forearm.

To do so, we measure the range of pronation of the healthy forearm and calculate the minimal distance between the vectors representing ulna and radius of our kinematic model. The range of rotation of the human forearm increases by the natural bending of the bones, especially of the radius. Although our model uses straight vectors, we consider this effect by calculating the distance of the vectors representing the healthy forearm at maximal pronation, which naturally can only be achieved through bending of the radius. Therefore, our calculation method serves as a type of normalization for the influence of the bending of the bones. With this value and the known size of the patient's bones taken from the X-ray-pictures we calculate the distances between the forearm bones in the angulated case as a function of α and stop, when reaching the minimal distance of the healthy arm.

2.2.1. Angulated ulna

To go further from this point, a model for the system with angulations is needed. To achieve this an extended vector loop, that includes one additional-vector for every angulation is introduced. The parameters k_1, k_2 and k_3 identify the angulation in the local coordinate-system of the fractured bone and are chosen to be taken directly from the X-ray-pictures. The local x-component k_1 can be measured from a.p. X-ray. It is defined as positive if it points in direction of the thumb. The local y-component k_2, taken from both the a.p. and side pictures is measured from the elbow to point A in supination. The z-component k_3, visible in the side picture is positive if the angulation is in palmar direction. These vectors are depicted in Fig. 3 along with one angulation of the ulna.

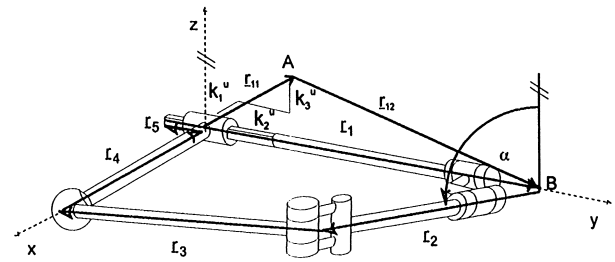

Fig. 3. Vectors of the angulated ulna. The vector r_1 is replaced by the vectors r_{11} and r_{12}.

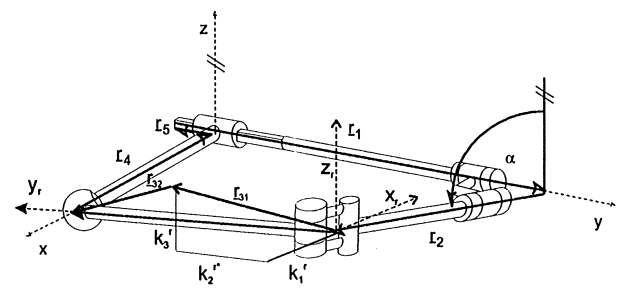

Fig. 4. Vectors of the angulated radius. The vector r_3 is decomposed into the vectors r_{31} and r_{32}.

We introduce the new vectors $\mathbf{r}_{11}$ and $\mathbf{r}_{12}$ in Fig. 4. $\mathbf{r}_{11}$ and $\mathbf{r}_{12}$ meet the following condition for every α:

$$\mathbf{r}_1(\alpha) + \mathbf{r}_5(\alpha) = \mathbf{r}_{11}(\alpha) + \mathbf{r}_{12}(\alpha). \tag{21}$$

We find the initial condition of $\mathbf{r}_{11}$ as

$$\mathbf{r}_{11}(\alpha = \alpha_s) = \begin{pmatrix} -k_1^u \\ k_2^u \\ k_3^u \end{pmatrix}. \tag{22}$$

Using Fig. 3, (5), (20) and (22) we obtain

$$r_{11_y}(\alpha) = \frac{k_2^u}{l_1}(r_{1_y} + r_{5_y}) = \frac{k_2^u}{l_1}\left(l_1 + l_2\left(\frac{l_1}{l_2} - \sqrt{\frac{l_1^2}{l_2^2} - 2(1 - \sin(\alpha))}\right)\right). \tag{23}$$

Only the y-values of $\mathbf{r}_{11}(\alpha)$ is dependent of α, hence,

$$\mathbf{r}_{11}(\alpha) = \begin{pmatrix} -k_1^u \\ r_{11_y}(\alpha) \\ k_3^u \end{pmatrix}. \tag{24}$$

With (5) and (20) the position vector of point B amounts to

$$\mathbf{r}_B(\alpha) = \mathbf{r}_1(\alpha) + \mathbf{r}_5(\alpha)$$

$$= \begin{pmatrix} 0 \\ l_2\left(-\sqrt{\frac{l_1^2}{l_2^2} - 2(1-\sin(\alpha))} + \frac{2l_1}{l_2}\right) \\ 0 \end{pmatrix}. \tag{25}$$

$\mathbf{r}_{12}(\alpha)$ is the difference between $\mathbf{r}_B(\alpha)$ (25) and $\mathbf{r}_{11}(\alpha)$ (24):

$$\mathbf{r}_{12}(\alpha) = \mathbf{r}_B(\alpha) - \mathbf{r}_{11}(\alpha)$$

$$= \begin{pmatrix} k_1^u \\ \left(1 - \frac{k_2^u}{l_1}\right) l_2\left(-\sqrt{\frac{l_1^2}{l_2^2} - 2(1-\sin(\alpha))} + \frac{2l_1}{l_2}\right) \\ -k_3^u \end{pmatrix}. \tag{26}$$

2.2.2. Angulated radius

The case of the angulated radius is more complicated, because the radius performs a spatial motion, whereas the ulna moves only in y-direction. To handle this case we define the local coordinate-system of the radius (Fig. 4). The index r indicates the local coordinate-system of the radius:

$$\mathbf{e}_y^r = \frac{\mathbf{r}_3}{|\mathbf{r}_3|},$$

$$\mathbf{e}_z^r = \frac{\mathbf{r}_2 \times \mathbf{r}_1}{|\mathbf{r}_2 \times \mathbf{r}_1|},$$

$$\mathbf{e}_x^r = \mathbf{e}_y^r \times \mathbf{e}_z^r. \tag{27}$$

Now, it is easy to describe $\mathbf{r}_3$ and the additional vectors $\mathbf{r}_{31}$ and $\mathbf{r}_{32}$ in the new coordinates.

$$\mathbf{r}_3^r = l_1 \begin{pmatrix} 0 \\ 1 \\ 0 \end{pmatrix}, \tag{28}$$

$$\mathbf{r}_{31}^r = \begin{pmatrix} k_1^r \\ k_2^{r*} \\ k_3^r \end{pmatrix}, \tag{29}$$

where

$$k_2^{r*} = l_1 - k_2^r \tag{30}$$

and

$$\mathbf{r}_{32}^r = \begin{pmatrix} -k_1^r \\ k_2^r \\ -k_3^r \end{pmatrix}. \tag{31}$$

Using (27), (29)–(31) can be transformed as

$$\mathbf{r}_{31} = \mathbf{r}_{31}^r \cdot \mathbf{e}_r \tag{32}$$

and

$$\mathbf{r}_{32} = \mathbf{r}_{32}^r \cdot \mathbf{e}_r. \tag{33}$$

The model can easily be expanded to deal with a double-fraction of ulna and radius by combining (6), (8), (24), (26), (32) and (33).

3. Results

We learn from Weinberg et al. (1997) that the amount of evasive angle of the ulna and radius (Fig. 1 — right half) relative to its supination position is 7.36° on average. This evasive motion in our model is performed by the extension of r_5 (Fig. 2). This translation can easily be recalculated for the natural evasive movement. By using a typical adults relation of 8:1 for the length of the forearm-bones compared to their distance in full supination position, we find a length increase of 3.1% which is equal to 7.2° of evasion rotation.

Hence, our kinematic model is in good agreement with the measured values of the MRI-study.

Furthermore, we will discuss two examples to show the reliability of our prognoses.

1. The first patient is female and five-years old has a left-hand-side forearm fracture of the ulna. From the a.p. X-ray-pictures we measured $l_1 = 153$ mm (length of the radius), $l_2 = 14.1$ mm (diameter of the capitulum radii, which we use as a measurement for l_2) and the dorsal angulation of the fracture $k_1 = -3.5$ mm. From the side- X-ray-picture we find the distance from the fracture to the elbow $k_2 = 46.7$ mm and the angulation of the ulna towards the radius $k_3 = -3.5$ mm.

   The range of motion of the healthy arm amounts to 80° in pronation direction. The angulation of the ulna does not limit the patients range of motion. By using our model for the broken ulna we calculated a range of motion of 80° in pronation direction, which is seen in reality.

2. The second example is a 31-year old male with a radius fracture on the right forearm. The length of the radius amounts $l_1 = 259$ mm, the diameter of the capitulum radii is $l_2 = 24$ mm, measured from the a.p. X-ray. The parameter of the fracture are $k_1 = -5$ mm (a.p. X-ray), $k_2 = 101$ mm and $k_3 = 17$ mm (k_1 and k_2 from side X-ray). The range of motion of the left forearm is 75° in pronation direction. The range of rotation of the right arm is restricted to 0° in pronation direction. Calculating the range of motion using the equations for the broken radius yields 3° of pronation.

4. Discussion

In 1872, Duchenne (1949) described the motion of the ulna during pronation–supination as an arc of a circle, which involved first an extension, then a lateral motion and lastly a flexion of the ulna. This description of the ulna motion was substantiated in 1884 by Heiberg (1884) and Dwight (1884).

Although this fact was known long ago, many authors fixed the ulna when examining the forearm rotation. With this simplified assumption they found a fixed rotation axis for the pronation–supination motion. But for a correct description the motions of both forearm bones, radius and ulna are important.

New experiments like the MRI-studies performed by Nakamura et al. (1994) and Weinberg et al. (1997) with a moveable ulna describe the ulna motion from supination to pronation as the combined abduction and extension/flexion motion, which is a corroboration of the early results of Duchenne and Hieberg.

Furthermore, instead of a fixed rotational axis for the forearm rotation, a rotation-angle dependent screw-axis for the forearm rotation is depicted.

We expanded our kinematic model to the case of a broken ulna or broken radius. This novelty can be used to predict the effects of forearm fractures on the range of forearm motion. A comparison with a still small patient database showed that the calculating method for pronation comes very close to nature. We cannot make a statement for supination yet. The kinematic model is mainly based on MRI-studies at this stage. We are going to make experiments on dead probands for a further refinement of our model, especially for the angulated case.

A computer tool will be developed that predicts motion restrictions due to forearm fractures from knowledge in human forearm rotational kinematics before the best therapy is chosen, in respect to helping in the prevention of unnecessary operations and thereby cutting health service costs and patient risk.

Furthermore, the kinematic model could be used to for further investigations of the role of the humero-ulnar joint during pronation–supination. This could help to improve existing elbow-joint prostheses.

References

Duchenne, G. B. A. (1949). Physiologiy of Motion, Demonstrated by Means of Electrical Stimulation and Clinical Observation and Applied to the Study of Paralysis and Deformities. Lippicott, Philadelphia (translated by Kaplan, E. B.).

Dwight, T., 1884. The movements of the ulna in rotation of the forearm. Journal of Anatomy and Physiology 19, 186–189.

Green, N. E., & Swiontkowski, M. F. (1998). Skeletal Trauma in Children. Vol. 3, Saunders, London.

Heiberg, J., 1884. The movement of the ulna in rotation of the forearm. Journal of Anatomy Physiology 19, 237–240.

Kerle, H., & Frindt, M. (1997). Zur Kinematik eines biomechanischen Modells für den menschlichen Unterarm. Proceedings of Getriebetechnik: Warnemünde, Rostock, Germany. pp. 115–123 (in German).

Kuderna, H. (1980). Zusammenhang zwischen Achsenfehlern und Funktionseinschränkungen nach Vorderarmfrakturen. Unfallchirurgie 6(1), 7–13 (in German).

Nakamura, T., Yabe, Y., & Horiuchi, Y. (1994). A biomechanical analysis of pronation–supination of the forearm using magnetic resonance imaging: dynamic changes of the interosseous membrane of the forearm during pronation–supination. Nippon Seikeigekagakuai Zasshi, Japan (in Japanese).

Nilsson, B.E., Obrant, K., 1977. The range of motion following fracture of the shaft of the forearm in children. Acta Orthopaedica Scandanavia 48, 600–602.

Weinberg, A.-M., Helm, M.B., Rzesacz, E., Reilmann, L., Kerle, H., & Reilmann, H. (1997). Can a limited pro- and supination caused by axis-deformation of the forearm-bones be predicted using computer-simulation? Computer Assisted Radiology and Surgery. Elsevier, Amsterdam. p. 1045.

Weiner, B. (1981). Schaftbrüche am Unterarm im Kindesalter. Thesis, Klinikum rechts der Isar, München, Germany (in German).